LA-UR-00-3781
Approved for public release;
distribution is unlimited.

Title:

ENVIRONMENTAL SITE CHARACTERIZATION UTILIZING AERIAL PHOTOGRAPHS AND SATELLITE IMAGERY: THREE SITES AT LOS ALAMOS NATIONAL LABORATORY, NEW MEXICO

Author(s):

Paul Pope, Naomi Becker, Ed Van Eeckhout and Cheryl Rofer
Los Alamos National Laboratory, Los Alamos NM 87545
Nancy David
Veridian ERIM International, 1570 Pacheco St., Suite E-13, Santa Fe, NM 87505
John Irvine
SAIC, 20 Burlington Mall Road, Suite 130, Burlington, MA 01803

Submitted to:

http://lib-www.lanl.gov/la-pubs/00818244.pdf

Los Alamos National Laboratory, an affirmative action/equal opportunity employer, is operated by the University of California for the U.S. Department of Energy under contract W-7405-ENG-36. By acceptance of this article, the publisher recognizes that the U.S. Government retains a nonexclusive, royalty-free license to publish or reproduce the published form of this contribution, or to allow others to do so, for U.S. Government purposes. Los Alamos National Laboratory requests that the publisher identify this article as work performed under the auspices of the U.S. Department of Energy. Los Alamos National Laboratory strongly supports academic freedom and a researcher's right to publish; as an institution, however, the Laboratory does not endorse the viewpoint of a publication or guarantee its technical correctness.

FORM 836 (10/96)

ENVIRONMENTAL SITE CHARACTERIZATION UTILIZING AERIAL PHOTOGRAPHS AND SATELLITE IMAGERY: THREE SITES AT LOS ALAMOS NATIONAL LABORATORY, NEW MEXICO

Paul Pope, Naomi Becker, Ed Van Eeckhout and Cheryl Rofer
Los Alamos National Laboratory, Los Alamos NM 87545
(http://www.lanl.gov/tsa/tsa4/enviro/char.html)
Nancy David
Veridian ERIM International, 1570 Pacheco St., Suite E-13, Santa Fe, NM 87505
John Irvine
SAIC, 20 Burlington Mall Road, Suite 130, Burlington, MA 01803

KEY WORDS: Environmental Monitoring, Photogrammetry, Remote Sensing, Image Processing, GIS, Solid Waste, Hydrology

ABSTRACT

The proper treatment and characterization of past hazardous waste sites is becoming more and more important as world population extends into areas previously deemed undesirable. Historical aerial photographs, past records, and current airborne and satellite imagery can play an important role in characterizing these sites. These data provide clear insight into defining problem areas in preparation for further characterization or remediation. Three such areas at Los Alamos National Laboratory are discussed in this paper:

i. wastes buried in trenches,
ii. surface dumping, and
iii. surface water modeling of contaminated sediment.

INTRODUCTION

Los Alamos National Laboratory (LANL), located in Northern New Mexico (Fig. 1), has been engaged in cleaning up many of its hazardous waste sites created during the last 50 years of weapons development. This effort has utilized a variety of techniques: past records, current and historical aerial photographs, satellite and airborne remote sensing, as well as ground surveys, have all played an important role. The effective combination of these data can provide clear insight into defining problem areas, as well as indicating where more detailed characterization information might be required. In this paper historical aerial photographs, airborne thermal and infrared data, and certain ground measurements are combined to define the surface extent of pits, trenches, and the distribution of surface contaminants.

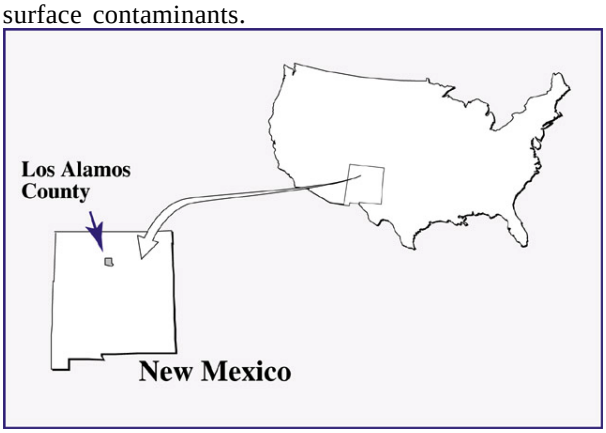

Fig. 1. Location of Los Alamos County, New Mexico

The waste sites evaluated at LANL, known as Materials Disposal Areas F (MDA-F) and M (MDA-M), consist of hazardous waste buried in trenches and dumped on the surface. The locations of MDA-F and MDA-M are shown on Fig. 2, which displays the boundary of Los Alamos overlaid on a Landsat false color image. Potrillo Canyon, the third area under discussion, is noted as well. LANL encloses about 43 square miles. The towns of Los Alamos and White Rock are shown in the image at the top and lower right respectively. The Rio Grande River crosses from the middle right to middle bottom of the image. The area has high relief, ranging from 10,000 ft in the Jemez Mountains above Los Alamos to about 6600 ft at White Rock. LANL is located on the flanks of the Jemez Caldera, a volcano that last erupted over 1 million years ago. The mesas and plateaus are composed mostly of volcanic tuff, and the climate is semi-arid.

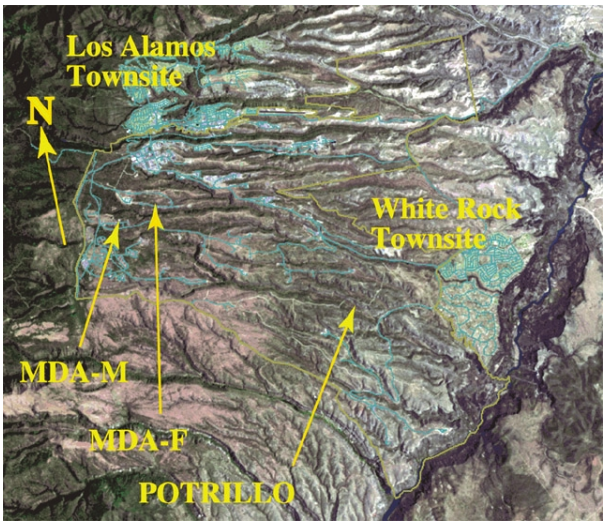

Fig. 2. Boundary of LANL overlaid on Landsat false color imagery showing waste site locations and paved roads.

MDA-F

The general area around MDA-F was used during World War II for the development of an implosion weapon, as part of the Manhattan Project activities. Waste disposal activities at MDA-F began in 1946 when the Laboratory Director ordered the construction of disposal pits for the burial of classified objects, and continued through 1952. It is believed that, in addition to classified objects, spark gaps containing ^{137}Cs, metal parts, tuballoy, primacord, and possibly high explosives were buried at MDA-F. The number and location of these trenches and pits were unknown. The total depth of burial was also not known, but from the available records and interviews with participants, it was believed to be about 3 m. Since the exact location, number, and extent of the trench and pit boundaries were uncertain, it was important to identify and delineate the disposal boundaries in this area to aid in sampling and remediation activities.

Figure 3(a) shows a 1991 orthophoto of the MDA-F area, with the boundaries of suspected trenches overlaid on the photo. Based on these boundaries, a magnetic gradient survey area was defined as shown on Fig. 3(b), and overlaid on a 1958 photograph. Note that the pits and trenches appear to extend beyond the fence lines shown in Fig. 3(a). Because it seemed that the pits and trenches did extend farther than originally thought, a study to evaluate historical photographs of the area was initiated.

Fig. 3(a). 1991 orthophoto of MDA-F.

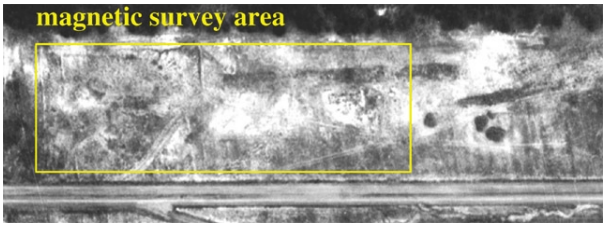

Fig. 3(b). 1958 matched photo of MDA-F.

Historical Imagery of MDA-F

Historical aerial photographs were digitally scanned in order to perform on-screen computer change detection. The digital analysis of these photographs

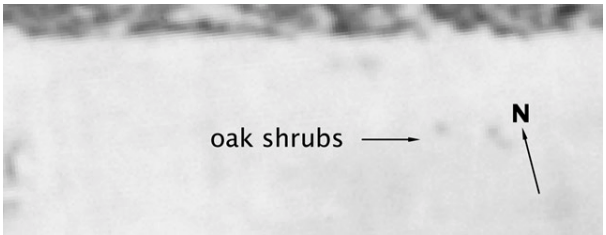

Fig. 4(a). 1935 image of MDA-F area.

Fig. 4(b). 1946 image of MDA-F area.

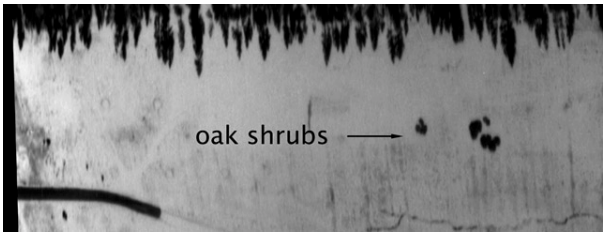

Fig. 4(c). 1949 image of MDA-F area.

Fig. 4(d). 1958 image of MDA-F area.

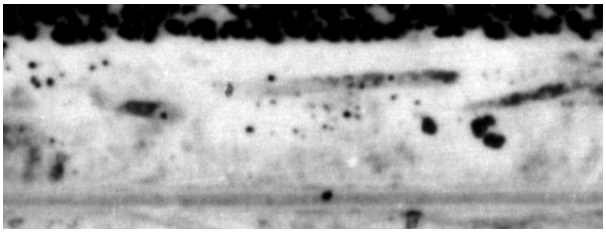

Fig. 4(e). 1972 image of MDA-F area.

Fig. 4(f). 1991 master image of MDA-F area.

allowed disparate views of the site to be transformed so that they matched in scale, orientation, and extent. This was especially useful for oblique photographs of the site. The coregistered images were studied individually and collectively to identify features which were indicative of human activity at the site and to provide a physical history of natural and human induced changes. The images used are shown in Fig. 4(a)-(f). Note the clump of scrub oaks that are common to all images.

The coregistered images were then imported to a GIS and geographically coded to a common coordinate system. The GIS was used to extract the boundaries of features such as suspected trenches and disturbed soil. The boundaries of disturbed ground, access routes, the main disposal trench, and three other suspected trenches were vectorized from the imagery by on-screen digitizing. These boundaries were overlaid on the most recent image of the site to display the historical characterization features within the context of how the site appears now. This preliminary analysis formed a basis for planning and comparing the results from other surveys of the site. The major trenches found are shown on Fig. 5. Further details of this analysis can be found in Pope and others, 1996.

Thermal and Infrared Data

Imagery from an airborne thermal infrared and multispectral survey, performed by Bechtel/Remote Sensing Laboratory of Nellis AFB, was also made available for analysis (Bell et al., 1996). The imagery was imported to the GIS and georeferenced. Various enhancements were calculated, including linear contrast stretches, edge enhancements, and principal components analysis. Information about trench locations and disturbed ground was extracted from the enhanced imagery. This information matched well with the analysis of the historical aerial photographs and the magnetic gradient survey.

Fig. 5. Suspected trenches and pits within the area of interest. Note the two large trenches. The one on the right wasn't suspected until the historical photography was inspected.

Figure 6 shows some of the thermal data over MDA-F. The cold and more moist spots are darker in this imagery. In order to verify this, two transects were established across the suspected easternmost pit, as shown in Fig. 7. Both moisture and temperature measurements across these transects indicated differences from the surrounding area. In general, soil moisture content in the trenches was twice as wet as the background and soil temperatures were lower. Figure 8 shows the lowering of temperatures at a 6 inch depth of burial in the middle of each trench compared to background.

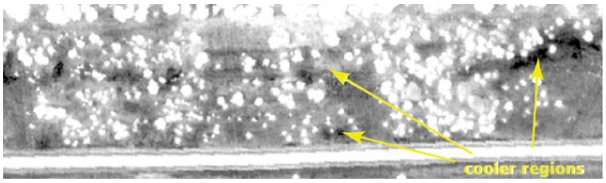

Fig. 6. Thermal imagery over MDA-F. The arrows note some particularly cooler and wetter locations, which appear to correspond to pits and trenches.

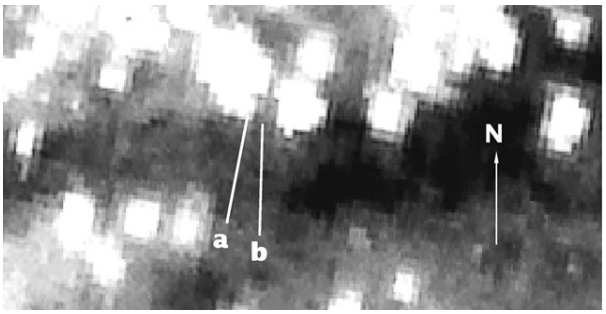

Fig. 7. Two transects across the easternmost pit, shown on thermal imagery. Background measurement to the east (right) of image.

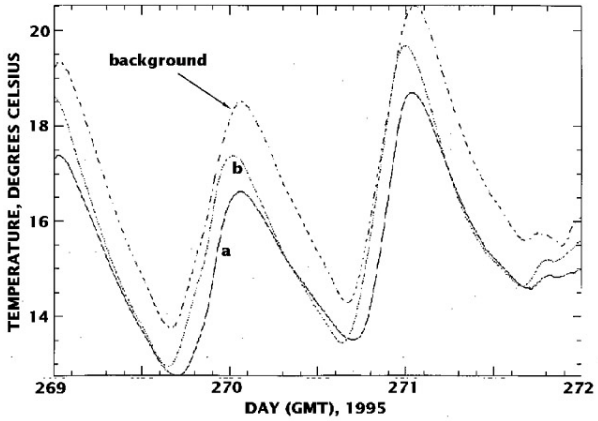

Fig. 8. Comparison of transect a and b temperatures with the background.

MDA-F Summary

Digital analysis of aerial photos at LANL allowed disparate views of a waste site to be transformed so that they matched in scale, orientation, and extent. Surface expression of old trenches can then be found more easily. Also, with additional data, such as infrared and ground based moisture and temperature,

confidence in the outlines of the trenches is strengthened.

MDA-M

According to internal information, which was scarce, the waste site known as MDA-M was used for surface disposal from 1948 until 1965. Inspection of the site revealed building demolition material and construction debris. Digital processing of historical photography was used to obtain a more informative site characterization.

Historical Imagery of MDA-M

Detailed analysis of historical photos for this site followed the same procedure as that described in the previous section, except that more photos were used. The use of more photos increased the temporal sampling available for determining the land use history of the site.

Internal and external archives were searched for aerial photographs, which bracketed and spanned the period of use of MDA-M for disposal. Photographs from 1935, 1947, 1951, 1958, 1960, 1964, 1972, 1976, 1986, and 1991 were used. For the sake of brevity, only a subset of these photos will be displayed in this paper.

The photographs were digitized with a flatbed scanner capable of 1200 dots per inch (dpi) optical resolution. The scanning resolution was adjusted for each photograph so that the spatial resolution was as close to one foot per pixel as possible. The 1991 image was georeferenced to New Mexico Central State Plane coordinates (NAD83) by using the corner tick marks on the orthophoto as control points. This image was used as a base image. All of the other images were resampled via an affine transformation to match this base image in scale, orientation, and extent. This reduced the planimetric distortions due to the combined effects of viewing geometry and terrain relief. The results of registering the historical images to the base image are shown in Figs. 9(a)-(f). Visual interpretation of these registered images through on-screen animation allowed the following land use history of MDA-M to be derived.

The 1935 image indicates that this area was an open space even before LANL was established (Fig. 9(a)). This open space most likely provided an easy opportunity for establishing a surface disposal site since no trees had to be removed. Many access trails created by homesteaders were evident. However, no major route to the site was detected in this image.

The history of vegetative cover at the site is very informative. Trees were removed to create a road into the area some time between 1948 and 1951. The width of this road does not appear to change significantly from 1951 to 1991. The construction of this road coincides with the first visible evidence of surface debris at the site in the 1951 image (Fig. 9(c)). Surface debris is not visible in the 1935, 1947, and 1948 images. Only forb cover, bare soil, and erosional patterns are evident on these images. Small trees begin to grow within the site and on top of the debris mounds starting in 1972. These trees are clearly evident on the 1991 image. This reclamation of a disturbed area by tree cover was also evident at MDA-F. This effect might be used to detect other lab areas which should be studied in more detail for evidence of disposal activity.

Surface disposal at the site is indicated by three distinct, east-west oriented mounds, which appear as darker, elongated features on all of the images after 1948 (Figs. 9(c)-(f)). These features have a mottled appearance and contain small, bright pieces of material. These areas change only slightly between 1951 and 1954, with evidence of debris deposition appearing on the western end of the northern and central mounds. Stereoscopic viewing of stereo pairs from 1951 and 1958 revealed significant movement of soil and material in several places. A much brighter material is deposited on the northwestern portion of the first mound between 1951 and 1954. Of special note is the fact that these mounds do not change significantly between 1954 and 1991, which suggests that the majority of the surface disposal was performed between 1948 and 1954. Neither pits nor trenches were detected at this site.

Changes in the drainage patterns across the site are also informative. Major changes in erosional patterns are apparent after the creation of a berm around the site. This berm was created between 1951 and 1958. The berm has restricted runoff from the northwestern portion of the site to travel close to the berm in a west to east fashion, where it eventually spills into the southern tributary of Pajarito Canyon. Some of the deep erosional patterns apparent on the 1947 image (Fig. 9(b)) reappear within the eastern portion of the central debris mound. However, the berm appears to have contained the majority of runoff within the site. The berm does not appear to have eroded significantly since 1958 and is readily apparent from 1958 till 1991 (Figs. 9(d)-(f)).

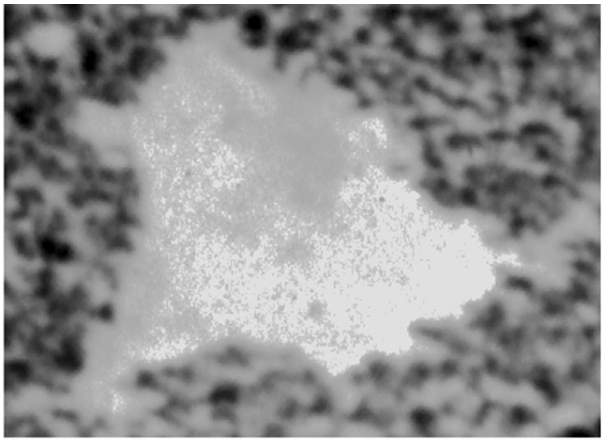

Fig. 9(a). 1935 image of MDA-M area.

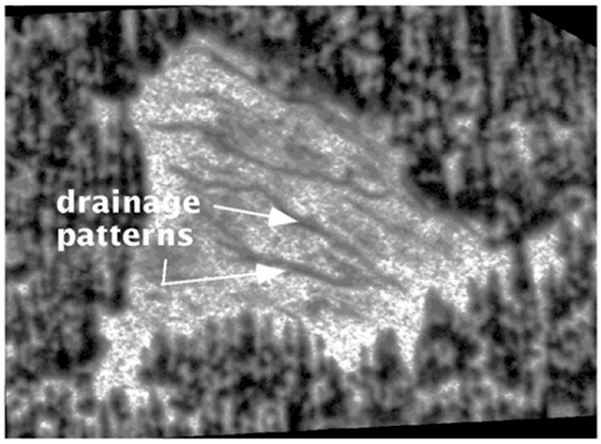

Fig. 9(b). 1947 image of MDA-M area.

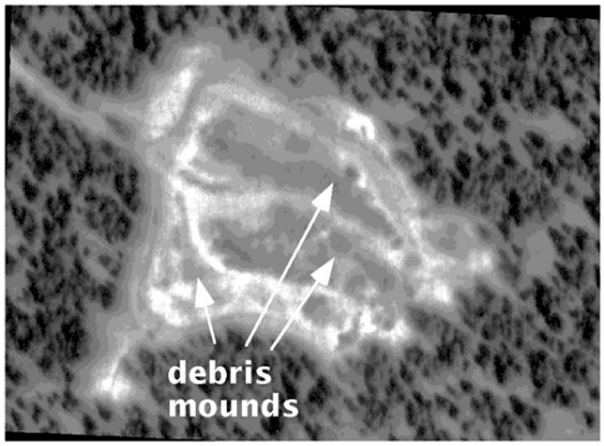

Fig. 9(c). 1951 image of MDA-M area.

Fig. 9(d). 1958 image of MDA-M area.

Fig. 9(e) 1974 image of MDA-M area.

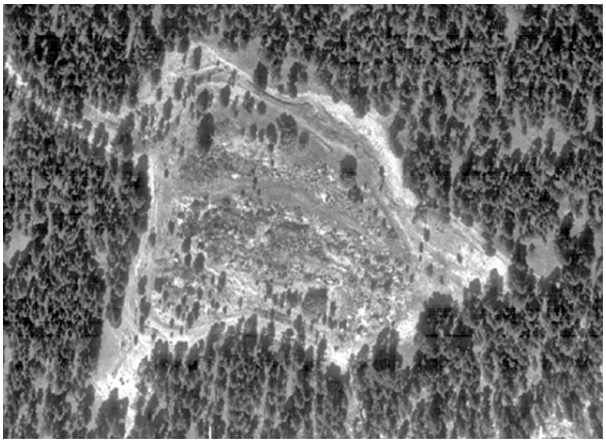

Fig. 9(f). 1991 master image of MDA-M area.

Several types of features were extracted from the registered historical images. These features were extracted by on-screen digitization of their boundaries as determined by visual interpretation of the digital images and stereoscopic viewing of stereo pairs. The 1947, 1951, and 1958 images were used to derive these features because they are indicative of the major changes which have occurred at the site, and they have good contrast and detail. Boundaries of the three debris mounds were extracted from the 1951 and 1958 images. Drainage patterns evident in the 1947 and 1958 images were traced. The top of the berm was digitized from the 1958 image. These vectors were overlaid on the 1991 base image to create an image-based

characterization map. This map allows the positions of the historical features to be compared within the context of current site conditions, and was a great aid to remediation fieldwork.

MDA-M Summary

The digital analysis of historical aerial photographs of MDA-M has enabled a detailed characterization of this waste site to be created. Providing a high degree of temporal sampling allowed various disposal activities and natural changes in the site to be more closely bracketed in time. For example, it is now known that the majority of disposal activity occurred between 1948 and 1954. This also allows internal documents, such as work orders for building demolition, to be more closely associated with disposal activity at the site. Careful attention to details in changes at the site aided in attributing these effects to various actors, both human and natural. Analysis of changes in drainage patterns at the site provided evidence for where soil-sampling efforts might be concentrated.

The historical photo analysis provided valuable information, which was used to clearly define the necessary remediation actions. Based on previous LANL remediation costs, the waste disposal cost alone for MDA-M was estimated to be $7.5 million. An improved remediation plan was created based on the information provided by the historical photo analysis. This made it possible to create a fixed-unit-price contract, and provided incentives to the contractor to reduce costs for waste disposal. A fixed-unit-price contract was made for the entire remediation, including waste disposal, at $1.5 million; a savings of $6 million. This cost is significantly less than the cost of one month's time from a single researcher, trained in image processing and aerial photo interpretation, required to perform the historical photo analysis.

POTRILLO CANYON WATERSHED

KINEROS, an event-driven model of surface runoff and sediment transport, was used to assess uranium transport for various rain events within the Potrillo Canyon watershed. This watershed contains multiple firing sites and known surface contamination. The KINEROS model includes input parameters related to the size and slope of watershed components, vegetation, and soil conditions. One distinct set of model inputs was derived from remotely sensed visible and multispectral imagery to assess the potential surface runoff and contaminant transport and compare with results derived from site-specific, ground-based knowledge. Depleted uranium, used in weapons testing activities at LANL since the mid-1940's, was used as a tracer of sediment movement.

Ground Truth Data

Potrillo Canyon is small, about 7.8 km^2, and has an average gradient of three percent. The watershed is characterized by flat mesa tops leading to nearly vertical canyon walls that terminate in large talus piles of volcanic tuff boulders. Vegetation varies significantly from a covering of Ponderosa pine forest at elevations over 2100 m, to a piñon-juniper community near the watershed outlet. The soil cover on mesa tops is thin to absent, and ranges from thin to over 9 m in the canyon bottom. The watershed contains five firing sites (four active and one inactive).

From 1983 through 1990, samples of soil, sediment, and surface water were collected both spatially and temporally. Over 4100 measurements were made from a total of 750 samples. In 1994, a database was created containing sample location, physiography, and contaminant information (Becker and others, 1995). Analysis of duplicate samples indicated high laboratory accuracy for this data set. Collection circumstances were well documented. Summary statistics indicate that the mean uranium concentration in soil is 1.5. parts per million (ppm). By comparison, background concentrations of uranium in this region range from two to five ppm. These data, when combined with existing topographic, hydrographic, and soil physics information, were used to develop the KINEROS input parameters. The parameters are used to describe and model geometric, hydrologic, erosion, rainfall, sediment, channel and pond components of the watershed as it responds to rainfall, generates runoff, and ensuing sediment transport. The watershed is subdivided into discrete elements, over which rainfall, runoff, and sediment processes are simulated. A complete description of KINEROS can be found in Woolhiser and others, 1990.

Remotely Sensed Imagery

Imagery collected from an airborne Daedaleus sensor was processed and exploited to assess surface features and characteristics that influence surface runoff and sediment transport. Topographic information (elevation contours) was extracted from available USGS maps. The synergistic exploitation of visible and multispectral imagery provided localized information about geographic strata of the watershed, types and density of the vegetation, and indications of surface soil and rock conditions. By translating this information into specific parameter estimates, it could be input into the surface runoff model component of KINEROS.

Panchromatic and multispectral imagery was collected over the study area using the Daedalus 1268 multispectral scanner, which offers a source of

relatively high resolution (1 to 2 meter) imagery. The Daedalus sensor collects 12 spectral bands ranging from the visible portion of the spectrum to the long-wave infrared. Analysis of various band composites can reveal vegetation features, indications of soil moisture, and factors suggesting different surface materials.

The imagery analysis was performed primarily with softcopy data using Erdas Imagine. Imagery from various band composites was analyzed separately, then jointly, using conventional imagery analysis techniques. A supervised classification of the data categorized the regions of the watershed according to surface vegetation and soil characteristics. The four basic classes of trees, grass, rock, and soil influence the hydrologic parameters for KINEROS. In some cases, more subtle signatures, such as indications of differential soil moisture or rock types, were used to fine-tune the parameters. Visible imagery was used to assess the topography of the canyon and determine the location of the channels within the watershed. The topographic maps were used to delineate the watershed boundaries. Slight differences in the direction of the slope have a significant effect on the watershed boundary, and can be detected more easily on maps than on imagery. The KINEROS element boundaries were determined based on visual analysis of the slope direction and magnitude within the watershed using both the imagery and topographic maps. Additional information regarding ground cover for each element, expressed as the percentage of each element covered by trees, grass, rock, or soil, was determined using available imagery, and was used to help refine the hydrologic parameters such as saturated hydraulic and effective net capillary drive.

A series of multispectral composites of the region around the one firing site, Lower Slobovia, illustrate the contribution from different spectral regions. The natural color image (red, green, blue composite), Fig 10, provides a good overview of the area. Roads and trails stand out as bright linear features. The green vegetation is distinguishable from the stressed (brown) vegetation or bare soils.

Fig. 10. Daedalus natural color composite image.

The near-IR composite (near-infrared, red, and green), Fig. 11, indicates the biomass, useful for identifying the low-growing vegetation, such as grass and shrubs. These data were used in selecting hydrologic model parameters.

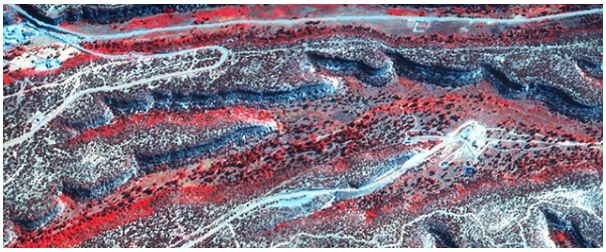

Fig 11. Daedalus Near-IR composite image.

Similar information, along with indications of soil moisture, is apparent in the SWIR composite (short-wave infrared, near infrared, and red), Fig 12.

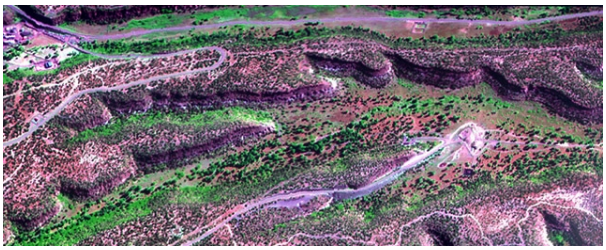

Fig 12. Daedalus SWIR composite image.

For example, the darker red surface areas in the discharge sink probably arise from the enhanced infiltration of runoff in this region (see Becker 1991, for detailed discussion on the discharge sink's hydrologic significance). Finally, the long wave thermal image, Fig 13, shows differences in radiance that arise from temperature or emissivity differences. This is particularly evident in the mesa cliffs, where the various geologic strata show differences in radiance. These data were used to distinguish soil type and establish soil physics and sediment properties.

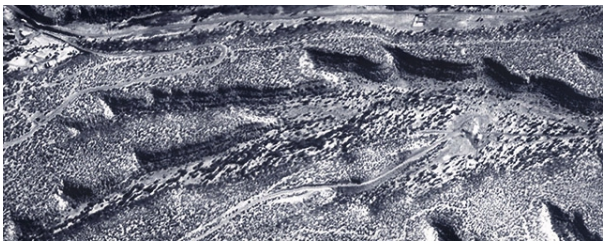

Fig 13. Daedalus thermal image.

Potrillo Canyon Discussion

Assuming that the ground-truth data is calibrated to approximate measured flows, the imagery data alone will under-estimate flow discharge. This is clearly demonstrated in the Two-Year storm case, Fig 14.

However, when the imagery data is augmented and modified with additional hydrologic knowledge, it is capable of reproducing flow discharges with a reasonable degree of accuracy.

The peak sediment discharge rate predicted by the imagery data is one-half to about one-third the value predicted by the ground truth data parameter set. When the total sediment production from all watershed elements, excluding the case where the imagery data is not modified by hydrologic knowledge of the watershed, is considered, the imagery data predicts sediment mass, which is about 70 to 80 percent of that predicted by the ground truth data set.

Uranium transport calculations on runoff from the Two-Year recurrence interval storm at the terminus of the watershed indicate slight uranium transport, ranging from 0.2 to nearly 0.5-kg uranium transported in the annual flood. These predictions are comparable to other inferences on uranium transport in Potrillo Canyon watershed from other methods.

A comparison of model performance based on remotely sensed data to the model developed from site-specific information suggests that approximate estimates can be obtained through remote sensing, provided some general collateral information is also available. The model results offer valuable information about which portions of the watershed contribute the most to contaminant transport.

CONCLUSIONS

This paper has shown how imagery gathered by aerial and remote sensing surveys can significantly aid waste site characterization studies. Enhanced characterizations of three waste sites at LANL were obtained by utilizing photographs and digital images gathered by airborne systems. Image processing techniques and geographic information systems were useful for analyzing and combining data from these systems into a form which could be used more easily for visual interpretation and cartographic work. Overhead imagery provides a synoptic view in the spectral, spatial, and temporal dimensions. Overhead imagery is not a replacement for ground truth. Rather, these data allow limited ground truth to be extended in each of these dimensions so that a more complete characterization can be formulated.

ACKNOWLEDGMENTS

Special thanks go to Ray Brewer, Larry Creamer, Eddie Tafoya (all from LANL) for helping with site analysis and historical photo retrieval. The assistance of Lee Balick, from the Bechtel Remote Sensing Lab, for infrared images and Kathleen Allyn for photo interpretation is also gratefully acknowledged. Funding for this work has been provided by the LANL Environmental Restoration program, the DOE Government Applications Task Force, and internal LANL funds.

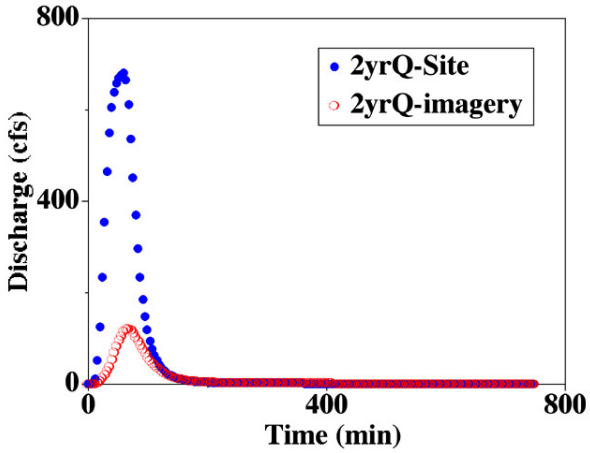

Fig 14. Comparison of ground-based vs. imagery-based hydrographs for the 2-yr recurrence interval.

REFERENCES

N. BECKER, *Influence of Hydraulic and Geomorphologic Components of a Semi-Arid Watershed on Depleted Uranium Transport*, Ph.D. dissertation to the University of Wisconsin, Los Alamos National Laboratory report LA-UR-93-2165 (1991).

N. BECKER, N. DAVID, J. HOOPES, *Hydrologic Transport and Ecosystems Investigation Results of Phases I and II Sampling Strategies, Correlation Between Elements and Hydrologic Modeling of a Large Metals Data Set in Potrillo Canyon Watershed*, Los Alamos National Laboratory Report LAUR-95-2800 (1995).

R. BELL, J. IRVINE, N. BECKER, T. EVERS, A. KING, M. PENDERGAST, J. SMYRE, E. VAN EECKHOUT, P. WEBER, Bell, R., *Final Report on the Government Applications Task Force*, Dept. of Energy Pilot Project (1996).

P. POPE, E. VAN EECKHOUT, C. ROFER, "Waste Site Characterization Through Digital Analysis of Historical Aerial Photographs," *Photogrammetric Engineering and Remote Sensing*, **62**, 12(1996).

D. WOOLHISER, R. SMITH, D. GOODRICH, *KINEROS, A Kinematic Runoff and Erosion Model: Documentation and User Manual*, U.S. Department of Agriculture, Agricultural Research Service ARS-77, (1990).